J Therm Anal Calorim (2011) 104:849–858
DOI 10.1007/s10973-011-1288-0

Reactivity of cement mixtures containing waste glass using thermal analysis

L. M. Federico · S. E. Chidiac · L. Raki

CTAS2010 Conference Special Chapter

Abstract A laboratory study was undertaken to compare the performance of waste glass as a supplementary cementitious material (SCM) to traditional SCMs at the same particle size and level of replacement in both high and low alkali cement paste. The consumption of $Ca(OH)_2$ as measured by differential thermal analysis (DTA) is used as an indicator of reactivity. The DTA results of the pastes aged to 150 days are presented, and indicate that glass reactivity is similar to ground-granulated blast furnace slag (GGBFS) and lower than silica fume (SF) at comparable particle sizes. Alkali–silica reaction (ASR) is not present for particle sizes below 100 μm, but is induced by agglomeration of the glass particles and is observed by fluorescence in optical microscopy images. Scanning electron microscopy (SEM) and energy dispersive X-ray spectroscopy (EDS) are used to compare the microstructural properties of the SCMs and measure the chemical composition of the reaction products. The alkalinity of the cement was found to influence the nature of composition as observed by thermal analysis, and the temperatures at which their reactions occurred.

Keywords SCM · ASR · Pozzolan · Waste glass · DTA · Alkalinity

L. M. Federico (✉) · S. E. Chidiac
Department of Civil Engineering, McMaster University, Hamilton, ON, Canada
e-mail: federilm@mcmaster.ca

L. Raki
Institute for Research in Construction, National Research Council Canada, Ottawa, ON, Canada

Introduction

Supplementary cementitious materials (SCM) are used as cement replacement in concrete to improve a number of concrete properties, including durability, ultimate strength, workability, heat of hydration and permeability [1–4]. These properties are developed through pozzolanic reaction between amorphous silica in the SCMs and Portlandite, ($Ca(OH)_2$), released during cement hydration and formation of insoluble calcium silicate hydrates (C–S–H) [5].

Waste-based and industry by-product SCMs, such as silica fume (SF) and ground-granulated blast furnace slag (GGBFS), can also offset a portion of greenhouse gas (GHG) emissions that would result from the production of an equivalent amount of Portland cement from raw materials. For each tonne of Portland cement powder produced, a nearly equivalent amount of GHG is produced [3]. In 2001, the Canadian production of GHG per tonne of cement was 0.8 tonnes, which is similar to the 1996 value [6], and so there is still significant opportunity for environmental improvement.

Other potential SCMs include natural products, domestic, industrial and agricultural waste sources and demolition waste [7]. A post-consumer waste material which has yet to achieve the status of a commonplace SCM is bottle glass. This material is collected in municipal waste streams, and although glass is highly recyclable, the mixing of broken pieces can result in a reduction in the value of the waste product, as it cannot be separated by colour once this level of mixing has occurred. For this reason, recycled glass often ends up in low value products, or else in a landfill [8–10]. The use of waste glass as a partial cement replacement is not new [11, 12] and a number of studies have explored different uses for it in concrete. However, it has yet to become a competitive product in the marketplace due to

many early reported challenges associated with its use. Some of these challenges include the production of an Alkali–silica reaction (ASR) gel in the presence of large particles of glass, the loss of early strength due to contamination [13], and the cost associated with processing and grinding waste glass [12].

The effects of particle size on reactivity of pozzolanic SCMs and glass has been demonstrated [14, 15], where increased fineness led to an increase in early age compressive strength, even in the absence of activators. In some cases, the compressive strength of mortar bars made with glass powder as an SCM demonstrated a higher compressive strength than those made with an equivalent amount of fly ash [9, 16, 17]. Particle size is also influential in controlling the mechanism between alkali–silica and pozzolanic reactions. For glass particles with sizes below 300 μm, an ASR gel is less likely to be produced than with aggregate-sized particles, while particle sizes below 75 μm often demonstrate a pozzolanic reactivity according to the literature [10, 13, 18]. This general trend is not consistent, and depending on the composition of the glassy material, ASR can be exhibited even at very small particle sizes [19]. In other studies, a pessimum particle size was identified, where the maximum ASR expansion occurred at an intermediate particle size depending on the reactivity of the material [20, 21]. Both the reactivity of glass and its resulting reaction products have also been closely related to its chemical composition [22].

The pozzolanic and alkali–silica reactions follow similar mechanisms. Specifically, both require the dissolution of amorphous silica in an alkaline solution followed by the formation of a product bearing calcium, silica and alkali ions. The main difference between the two reactions is the properties of the resulting products, which can be loosely related to their chemical composition, namely the ratio of alkali to calcium and calcium to silica [23]. In a different study, a theory on the relationship between the chemical composition of the product and particle size of the waste glass suggested that the difference between ASR and pozzolanic products is conditioned by the particle size of the glass, but the controlling mechanism is unknown [24].

The goals of this paper are to determine whether or not waste glass would be comparatively reactive if ground to the same particle size as currently accepted SCMs, to determine the nature of the reaction, i.e. pozzolanic versus ASR, and to investigate the effect of cement alkalinity on the reactivity of the mixture.

Experimental

Six cementing powders were studied in this investigation. They included high alkali cement (HA), low alkali cement (LA), SF, GGBFS and glass powder. The composition of all raw materials, shown in Table 1, was determined by X-ray fluorescence. The two cement powders were obtained from Lafarge North America. The low alkali cement has a total Na_2O equivalence of 0.44%, and for the high alkali cement the Na_2O equivalence is 0.72%. SF from Norchem and GGBFS from Lafarge North America were obtained to serve as reference SCMs with distinctly different particle sizes.

Clear, unused wine bottles were the source of the glass. The glass was crushed by hand initially then further ground using a planetary grinder and a ring grinder to obtain two particle size distributions. The first, Glass 1, was intended to have a particle size distribution comparable to that of the SF, and the second, Glass 2, to that of the GGBFS. The particle size distributions of the SCMs and glasses are shown in Fig. 1. Although it was not possible to produce glass particles as fine as those of SF by grinding, a factor of nearly 10 was achieved to separate the glass meant to represent GGBFS from that of SF. Accordingly, the performance of the two glass groups was expected to be different. The mean particle size of Glass 1 and Glass 2 was 6.6 and 16.5 μm, respectively.

A Hitachi S-4800 Scanning Electron Microscope was used to evaluate the microstructure of the materials. Surface area for each sample was measured using the BET technique with a Nova 220e Surface Area and Pore Size Analyzer from Quantachrome Instruments. The surface areas, which are given in Table 2, reveal that glass at a comparable particle size has a lower surface area than GGBFS, and a much lower surface area than SF. These

Table 1 Material composition and characteristics

%	LA	HA	SF	GGBFS	Glass 1	Glass 2
SiO_2	20.41	19.65	94.90	35.85	71.59	72.06
TiO_2	0.32	0.24	<0.01	0.59	0.02	0.03
Al_2O_3	5.54	5.56	<0.01	10.52	1.78	1.81
Fe_2O_3	2.33	2.61	0.05	0.67	0.13	0.07
CaO	65.06	64.32	0.40	36.74	10.73	10.81
MgO	3.33	2.54	0.66	12.74	0.18	0.21
MnO	0.07	0.04	0.04	0.57	<0.01	<0.01
SO_3	2.63	3.20	0.11	3.60		
Na_2O	0.28	0.20	0.01	0.42	13.01	13.50
K_2O	0.24	0.79	0.63	0.47	0.40	0.40
LOI	2.19	3.46	3.01	1.23	2.32	1.00
Na_2O Eq.	0.44	0.72	0.42	0.73	13.27	13.76
C_3S	62.12	58.00				
C_2S	10.44	13.00				
C_3A	9.94	9.00				
C_4AF	6.84	8.00				

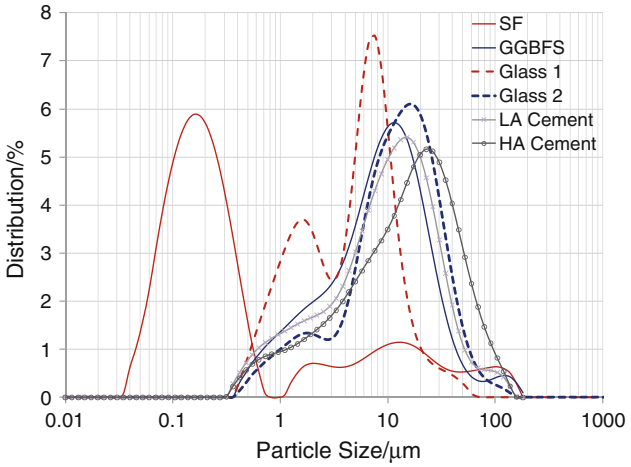

Fig. 1 Particle size distribution of cementing materials

results indicate that the shape of the glass particles differs from those of GGBFS and SF.

The scanning electron microscopy (SEM) images, shown in Fig. 2, are representative of the cementing materials. Glass 1, shown in Fig. 2b, was ground to simulate SF, Fig. 2a, but has more surface characteristics in common with GGBFS, Fig. 2c. The fine glass and GGBFS both share a combination of angular particles and foiled particles. The particles in Glass 2, shown in Fig. 2d, have a more consistent angular shape, and although they are similar in particle size distribution to GGBFS, they are not similar in particle shape and surface characteristics, since there are no apparent foiled particles. The lower surface area of Glass 2 is most likely due to the absence of the foiled particles seen in the GGBFS. These foiled particles would have a higher surface area than the relatively smooth and regularly angled particles observed for Glass 2, and therefore their absence in the glass may result in a lower surface area for similar particle size distributions.

Cement paste specimens were prepared by replacing 10% by mass of either LA or HA cement with SF, GGBFS, Glass 1, or Glass 2. The 10% replacement of waste glass is based on previous evidence which indicates that this is an optimum percent cement replacement in order to maintain or improve compressive strength [10, 17, 24]. A control mixture of 100% cement was also made for a total of 10 mixtures, Table 3. Each mixture was made with a water/binder ratio of 0.45 and cast into 100 mm long cylindrical plastic moulds, with diameters of 35 mm. The freshly cast mixtures were capped to prevent moisture loss and allowed to hydrate for 24 h before the moulds were removed. The specimens were stored at 23 °C and 95% minimum relative humidity until hydration was stopped at predetermined time intervals.

Samples from each mixture were freeze-dried to stop hydration with vacuum pumping while submerged in liquid nitrogen for 24 h, followed by 24 h drying in an unheated vacuum oven. While being stored for testing, mixture samples were sealed in a desiccator. Carbonation of the samples in the form of $CaCO_3$ was generally below 2.0% for low alkali mixtures and below 3.3% for high alkali mixtures. Simultaneous differential thermal analysis (DTA) was performed on crushed samples using a TA Q600 in nitrogen gas at 100 mL/min flow rate, with a ramping rate of 10 °C/min from room temperature to 1000 °C in an alumina pan. Sample size was 35 ± 5 mg. Each mixture was tested at 1, 14, 28, 91, and 150 days.

Data analysis

Thermal analysis results and trend lines are presented in Figs. 3, 4 and 5. The $Ca(OH)_2$ content was measured at different times as a percentage of the total sample mass, as shown in Fig. 3. By replacing 10% of the cement in each mixture with a SCM, 10% of the $Ca(OH)_2$ which would be produced during the hydration of Portland cement has been effectively removed. When the amount of $Ca(OH)_2$ in a mixture is measured to be less than 90% of the control, the additional consumption of $Ca(OH)_2$ can be attributed to another chemical reaction. A comparison of the mass loss to the original cement content (Fig. 4) shows that the low alkali mixtures have higher levels of $Ca(OH)_2$ than the equivalent high alkali mixture at the same age.

Figure 5 shows the relative $Ca(OH)_2$ consumption for all mixtures. At 28 days, only the mixtures containing SF have consumed significant amounts of $Ca(OH)_2$, while the other mixtures actually show increased amounts of $Ca(OH)_2$. This increase is expected as a result of the increased level of hydration from a higher relative water/cement ratio at the given water/binder ratio when SCMs replace a portion of the cement [25]. At 91 days, all mixtures have a reduced $Ca(OH)_2$ content below 90% of the control, but at 150 days, the levels of $Ca(OH)_2$ in the low alkali mixtures have increased. The high alkali mixtures generally maintain the same level of $Ca(OH)_2$ after 91 days. At early ages, all mixtures, except for those with

Table 2 Surface area

	LA	HA	SF	Glass 1	GGBFS	Glass 2
Surface area/m^2 g^{-1}	1.99 ± 0.10	2.57 ± 0.13	20.67 ± 1.03	2.32 ± 0.12	1.82 ± 0.09	1.59 ± 0.08

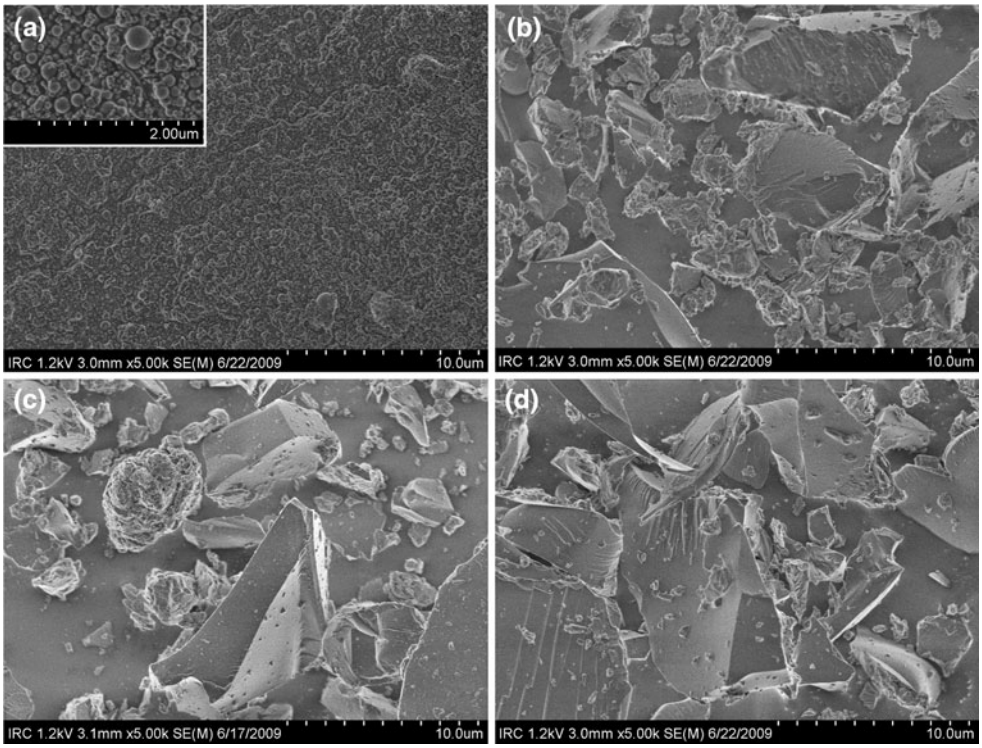

Fig. 2 SEM images of **a** SF, *inset* at ×5 higher magnification, **b** Glass 1, **c** GGBFS and **d** Glass 2

Table 3 Mixture compositions

Mixture #	Composition
1	90% LA cement + 10% SF
2	90% LA cement + 10% Glass 1
3	90% LA cement + 10% GGBFS
4	90% LA cement + 10% Glass 2
5	100% cement
6	90% HA cement + 10% SF
7	90% HA cement + 10% Glass 1
8	90% HA cement + 10% GGBFS
9	90% HA cement + 10% Glass 2
10	100% cement

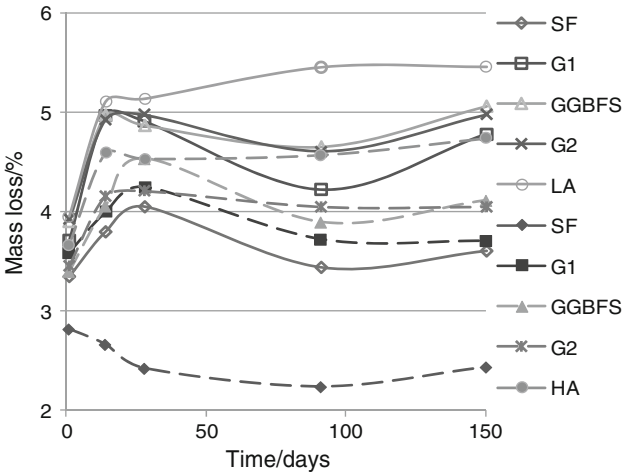

Fig. 3 Amount of $Ca(OH)_2$ mass loss determined by thermogravimetric analysis at 3, 14, 28, 91 and 150 days hydration for paste samples made with low alkali cement (*solid line*—LA) and high alkali cement (*dashed line*—HA)

SF, are experiencing hydration, leading to the increase in $Ca(OH)_2$, while at 90 days, $Ca(OH)_2$ is being consumed at a rate greater than that at which it is being produced by the hydration reaction. In the low alkali mixtures, the $Ca(OH)_2$ level recovers at 150 days. The production of $Ca(OH)_2$ from hydration or another source is taking place. Since typically Portland cement has reached 85% hydration by 100 days [26], the additional $Ca(OH)_2$ is unlikely to be a result of continued hydration.

The temperature ranges for each phase from the literature [27–35] were used to compare the thermogravimetric results at each age. Figure 6 shows the DTA of the mixtures at 28 days. It is apparent that certain phases are present only in low alkali mixtures, such as the phase between 165 and 175 °C, which is most likely ettringite at early ages and AFm or C_3AH_6 as hydration continues [36]. The phase located between 260 and 280 °C is also found only in the low alkali mixtures, which is another form of calcium aluminate hydrate, most likely cubic C_3AH_6 or C_4AH_{13} [36]. The temperature at which the $Ca(OH)_2$ peak occurs is lower for the high alkali mixtures. At 28 days, the

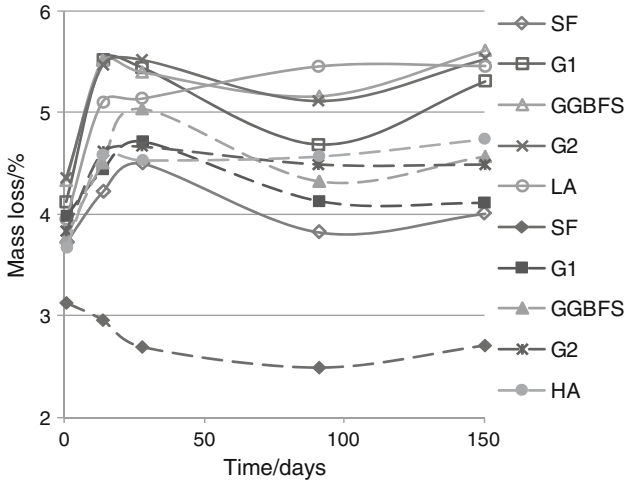

Fig. 4 Change in $Ca(OH)_2$ content per unit weight anhydrous cement for paste samples made with low alkali cement (*solid line*—LA) and high alkali cement (*dashed line*—HA)

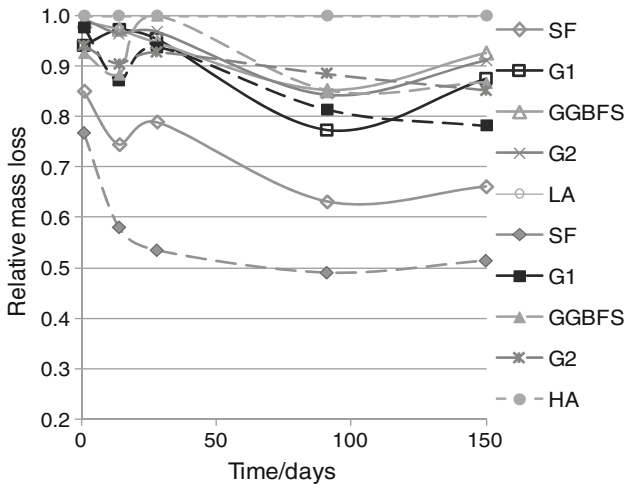

Fig. 5 $Ca(OH)_2$ consumption relative to control mixture for paste samples made with low alkali cement (*solid line*—LA) and high alkali cement (*dashed line*—HA)

average temperature at which the $Ca(OH)_2$ peak occurs for the low alkali mixtures is 448 °C, while for the high alkali mixtures, the average temperature is 444 °C. The peak which occurs between 650 and 750 °C is due to the decomposition of calcium carbonate ($CaCO_3$). Unlike the $Ca(OH)_2$, the $CaCO_3$ peak occurs at a higher average temperature (692 °C) for the high alkali mixtures than for the low alkali mixtures (676 °C).

Grain size can affect the temperature at which the peak occurs, where the peak temperature decreases as the crystal grain size decreases [37]. If higher alkalinity results in more but smaller $Ca(OH)_2$ crystals, this would account for the observed temperature differences between the $Ca(OH)_2$ peak in high and low alkali mixtures.

The decrease in the amount of $Ca(OH)_2$ observed in the thermogravimetric analysis can be at least partially attributed to one or both of two reactions, namely alkali silica reaction (ASR) and pozzolanic reaction. Both reactions consume $Ca(OH)_2$ and reactive silica to produce chemically similar products with very different physical characteristics. In determining which reaction is consuming $Ca(OH)_2$, a sample from each mixture was tested for the presence of ASR using the uranyl acetate staining method [38] according to ASTM C856 [39]. Freshly cut samples were exposed to uranyl acetate and observed under ultraviolet light with an optical microscope at 79 and 152 days. No fluorescence indicative of ASR was observed for control mixtures, mixtures containing GGBFS, SF, or Glass 2 (coarse glass). Mixtures containing Glass 1 (mixture 2 and mixture 7) demonstrated fluorescence and well-defined reaction rims at locations where fine glass was agglomerated together as a result of the grinding process. Some agglomerates, especially those which demonstrated fluorescence, experienced drying cracks typically associated with ASR. The location of the agglomerate did not appear to influence its characteristics, as several agglomerates with distinctly different properties were often observed in close proximity.

Some agglomerates of glass did not demonstrate fluorescence. In order to understand why some agglomerates would fluoresce and some would not, a more detailed analysis was performed and the composition of agglomerates ranging in size, colour, and level of fluorescence was examined using energy dispersive X-ray spectroscopy (EDS). The agglomerates were observed to range in diameter from ~25 to 2500 μm and to vary in colour from bright white to very dark grey under optical microscopy, and reaction rims were evident around most particles, as shown in Fig. 7.

The trend in both low and high alkali mixtures was that very small agglomerates, with an approximate area less than 0.01 μm^2, were more likely to fluoresce under UV light than larger agglomerates. Between 0.01 and 0.1 μm^2, agglomerates were less likely to fluoresce. At an area greater than 0.1 μm^2, agglomerates were just as likely to fluoresce as not to. The presence of this change in behaviour at intermediate sizes suggests that there is more than one process controlling the reaction of the agglomerate and the resulting product, similar to the pessimum effect of size observed in the literature [20, 40].

A typical Ca/Si ratio for ASR is 0.01–1.0 [41–44], and for C–S–H it is 1.5–2.0 [31, 45]. The glass used in the mixtures had a Ca/Si = 0.15, and a Na_2O equivalent of 13.27%.

Table 4 shows the range and average composition at various locations in and around the agglomerates in mixtures 2 and 7. Within the agglomerates, the Ca/Si ratio was

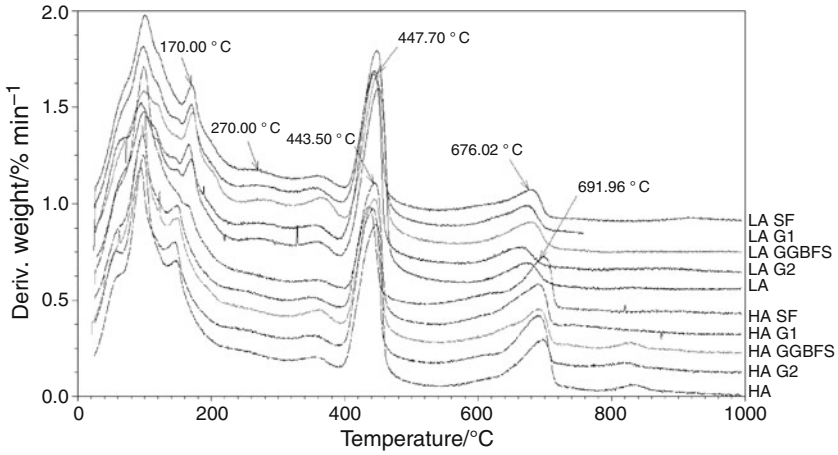

Fig. 6 Differential thermal analysis of LA and HA mixtures at 28 days

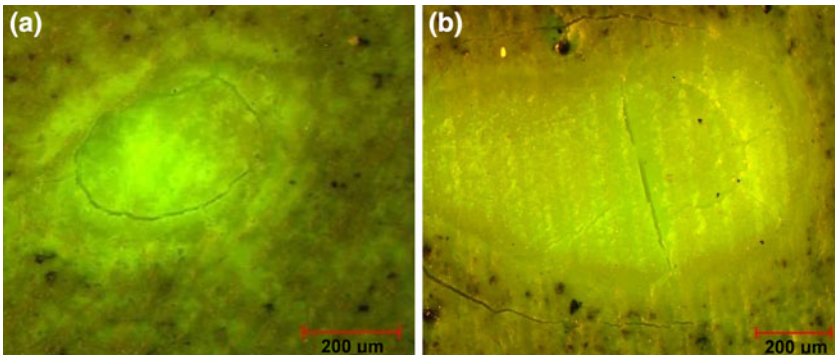

Fig. 7 Optical images for **a** mixture 2 (low alkali) and **b** mixture 7 (high alkali) with glass agglomerate, reaction rim and fluorescing

similar for both low alkali and high alkali mixtures. There was variability in the paste compositions for both mixtures near and away from the agglomerate. In general, as distance from the agglomerate increased, so did calcium content, while alkali content was variable. The silica content in the paste was significantly lower than in the agglomerates.

For the high alkali mixture, the centre gel and rim gel are compositionally comparable to ASR. The paste has a high Ca/Si ratio, and the Ca/Si ratio of the rim paste is much higher than that of the low alkali mixture. It is closer to C–S–H than ASR. ASR typically has a higher ratio of alkalis/Ca. The results in the table support the identification of ASR like material in all low alkali gel sites and in the centre and rim gel of the high alkali mixture.

In order to assess the cause of the variation in colours of the agglomerates, the compositions are compared in Fig. 8. Light agglomerates have Ca/Si ratios ranging from zero all the way to those typical of C–S–H (1.5–2), but also have alkali levels higher than would be expected in C–S–H. The medium and dark agglomerates demonstrate Ca/Si ratios and alkali contents of a low calcium C–S–H material similar to that observed in agglomerates of SF in other work [45]. The agglomerates with different coloured centres and rims show a composition which combines that of the light and dark agglomerates.

The colour of the agglomerates is loosely related to the tendency of the agglomerates to fluoresce under UV light when treated with uranyl acetate. Most agglomerates that fluoresced were light in colour, however being light in colour did not necessarily mean that fluorescing would occur, as many light agglomerates did not fluoresce. No dark agglomerates fluoresced; however fluorescing did sometimes occur in the light reaction rim surrounding dark agglomerates. Medium-coloured agglomerates and those which were light with a dark rim were just as likely to fluoresce as not, however no fluorescence occurred in dark rims.

From Fig. 9, agglomerates which demonstrated fluorescing had a lower Ca/Si ratio everywhere but in the gel side of the reaction rim. When slight fluorescence was observed, the composition at all locations was similar to the agglomerates that fluoresced but with slightly more calcium and more alkalis. When fluorescence was observed in the reaction rim, the alkali content was very high in the gel and rim, while Ca/Si was very high outside of the agglomerate, with very low alkali content. When no fluorescence was observed, the gel composition had only slightly higher Ca/Si and slightly lower alkali/Ca than the gel that fluoresced. The outer reaction rim and paste has a consistently high Ca/Si and low alkali/Ca when no fluorescence occurred.

Table 4 Atomic % composition of agglomerates and surrounding material

		Ca	Si	Na + K	Ca/Si	(Na + K)/Ca
LA						
Range	Centre gel	3.13–21.09	7.53–22.19	0.8–6.36		
	Rim gel	6.09–20.41	9.33–30.46	1.45–4.63		
	Rim paste	5.62–9.17	2.1–13.87	1.91–2.46		
	Paste	0–27.57	1.9–19.13	0.9–7.96		
Average	Centre gel	9.17	15.31	3.11	0.60	0.34
	Rim gel	10.82	17.16	2.76	0.63	0.26
	Rim paste	7.41	8.49	2.15	0.87	0.29
	Paste	11.93	6.20	2.66	1.92	0.22
HA						
Range	Centre gel	0–15.25	2.11–22.75	1.47–19.61		
	Rim gel	4.10–15.59	1.84–26.76	1.03–9.58		
	Rim paste	4.55–15	1.68–10.30	0.72–7.32		
	Paste	6.78–35.70	1.55–10.73	0–4.49		
Average	Centre gel	7.65	12.45	5.40	0.61	0.71
	Rim gel	7.52	12.72	4.45	0.59	0.59
	Rim paste	10.60	6.25	3.04	1.70	0.29
	Paste	13.13	5.12	2.17	2.56	0.17

Discussion

Although the glass was ground to achieve a particle size comparable to GGBFS and SF, the surface areas of the particles were different. This is especially true for SF, where the surface area was nearly ten times greater than that of the glass at the smallest particle size achievable through the grinding methods used. Mixtures composed of particles whose size is the smallest and surface area is the largest have the largest consumption of $Ca(OH)_2$ for all materials in both low and high alkali cement. This trend is well documented in the literature [46–50]. The observed formation of ASR in mixtures containing fine glass is due to the agglomeration of particles and not due to the particle size. Agglomeration of particles represents a high localised concentration of glass in comparison to the rest of the mixture. In areas where the glass was well distributed and in mixtures containing GGBFS, SF or coarse glass, no ASR gel formation was observed.

Although ASR occurred only at the location of glass agglomerates, it occurred regardless of the alkalinity of the cement. When ASR was observed, it occurred only in the vicinity of the agglomerates, and was not detected throughout the paste. Therefore, for a particle size distribution between 0.3 and 100 μm, ASR does not occur, and pozzolanic reaction takes place. At an agglomerate size ranging in area from 0.01 to 0.26 μm^2, ASR is found to occur in agglomerates, but is not guaranteed.

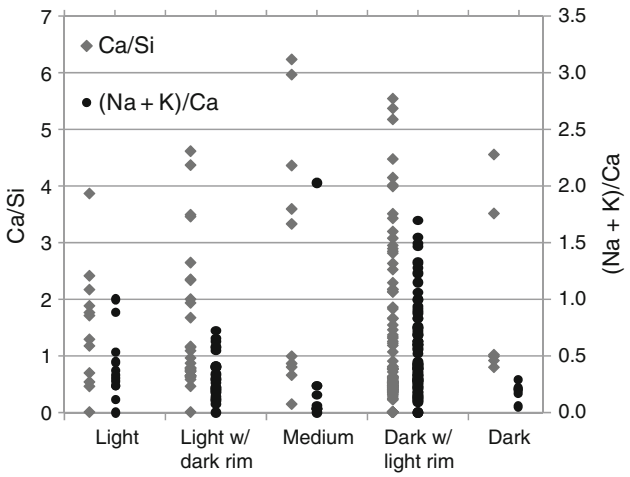

Fig. 8 Composition versus colour of agglomerate in mixtures 2 and 7

Upon further investigation, the agglomerates of varying sizes were found to have unique properties in terms of colour, fluorescence, and composition, which were not easily related to one another. Each colour of agglomerate observed has a unique composition. Those which were darker and less likely to fluoresce had lower alkali content and a Ca/Si ration similar to low calcium C–S–H. Those which were lighter and more likely to fluoresce had higher alkali contents, especially when fluorescing occurred only in the reaction rim. In low alkali cement mixtures, for which less data was obtained, the centre gel and reaction

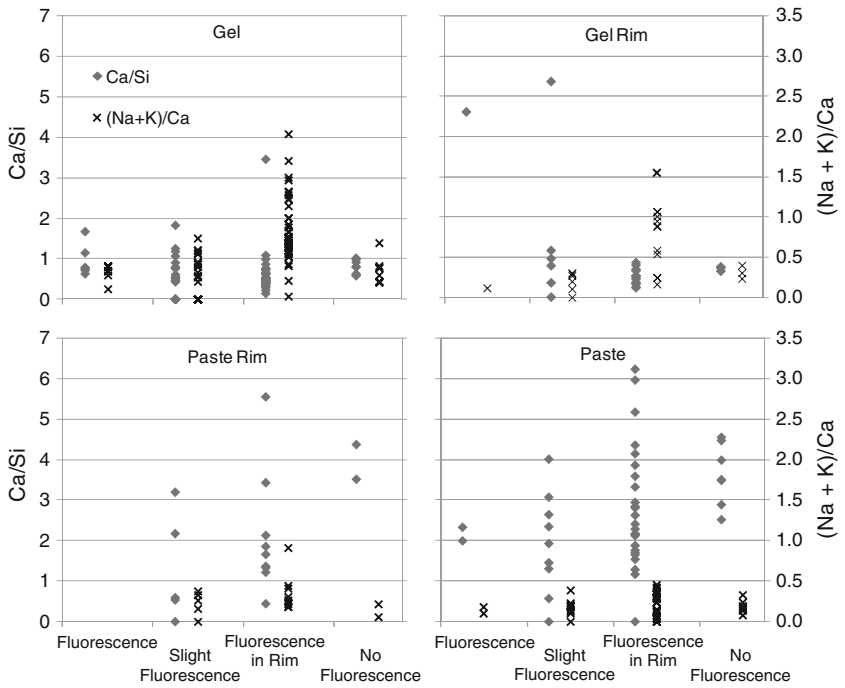

Fig. 9 Composition versus fluorescence of the agglomerate of interest for different locations in and around agglomerates

rims were compositionally similar to ASR, and the alkali content was generally mid range, decreasing towards the paste. In high alkali mixtures, a more distinct composition of ASR was observed in the interior reaction products and C–S–H in the outer rim and paste. The alkali content was much higher within the agglomerate, but was comparable to low alkali mixtures in the paste. The composition of the reaction rim not only influenced its colour and fluorescence, but that of the surrounding material. It is obvious from the results that calcium is being transported from the hydrating cement into the glass agglomerate, and alkalis are being relocated both throughout the gel and into the reaction rim. There are examples of agglomerates which seem to experience a discontinuity at the reaction rim which influences the resulting products. There are those which experience a very consistent ASR-type reaction within the agglomerate, seeming to leave the surrounding cement unaffected. There are also agglomerates which react with varying consistency to produce a low Ca/Si and relatively stable C–S–H type material. The cause of these distinctly different reactions is unknown; however, it does not appear to be strictly related to agglomerates size, location, or alkalinity of the cement. It is possible that an agglomerate with more surface area has a greater ability to react. Reaction at a greater rate allows for an increase in the exchange of calcium ions while the paste is still immature. This allows for a more evenly distributed gel with a composition closer to C–S–H than ASR [18], which was observed throughout the mixture, while the agglomerates induced local ASR [51]. Further study of the packing density and surface area of agglomerates may provide a distinction between the reactions observed.

There was an influential effect of alkalinity on the reactivity of the mixtures. When compared to conventional SCMs in low alkali cement, Glass 1 consumed less $Ca(OH)_2$ than SF at the same age. After 28 days, both showed a consumption of $Ca(OH)_2$ greater than 10% relative to the control mixture. Glass performed similarly to GGBFS in terms of $Ca(OH)_2$ consumption. In high alkali cement, SF was far more reactive than Glass 1. When compared to GGBFS, Glass 1 and Glass 2 in high alkali cement performed similarly, with consumption greater than 10% beyond 28 days for both mixtures, and no indication of ASR.

A comparison between hydration in low alkali cement and high alkali cement shows that there is generally more $Ca(OH)_2$ in the low alkali mixtures. Since the higher alkalinity increases the pH of the pore solution, decreasing the solubility of Ca, this result is expected [52]. Unlike the high alkali mixtures, the low alkali mixtures demonstrated an increase in $Ca(OH)_2$ at 150 days for all mixtures. Other researchers have postulated that increased $Ca(OH)_2$ levels observed in glass-bearing blends may be a result of glass constituents being incorporated into C–S–H in the place of Ca from the cement powder, resulting in excess $Ca(OH)_2$ in the pore solution [18].

There are two competing mechanisms which control the $Ca(OH)_2$ content in the paste: the hydration of cement powder, which produces $Ca(OH)_2$, and the pozzolanic or ASR reactions, which consume $Ca(OH)_2$. The difficulty

lies in distinguishing which reaction is consuming the $Ca(OH)_2$, and in following the reaction products for each reaction individually. If the rate of glass dissolution is greater than the production of either pozzolanic C–S–H or ASR gel, then the $Ca(OH)_2$ level may be increased due to substitution of sodium for calcium in the C–S–H [18]. This seems to be the case for the low alkali cement containing glass. For mixtures containing GGBFS, the additional $Ca(OH)_2$ may be the result of the hydraulic cementitious properties of the material [3]. In the case of the high alkali cement, pozzolanic or ASR reaction is taking place between 28 and 91 days, after which the $Ca(OH)_2$ levels stay relatively constant. At this point, the production of $Ca(OH)_2$ from hydrating cement has slowed significantly, as has any other reactions consuming $Ca(OH)_2$, or else they are balanced. If low alkalinity reduces the rate of glass dissolution, it is possible that the opportunity for pozzolanic and ASR reactions to take place in the young hydrating cement may have already passed before the silica could dissolve to significant completion.

The low alkali cement was observed to have more aluminate hydrate phases present than the high alkali cement for similar mixtures at the same ages. These additional phases may have been favoured as a result of the greater availability of $Ca(OH)_2$ in the low alkali mixtures. The temperature at which certain peaks occurred was observed to shift over time, and the $Ca(OH)_2$ peak for high alkali cement occurred at a lower temperature than that of the low alkali mixtures. Shifts observed in the peak temperatures over time and for different mixtures may be indicative of the development of different phases over time. Additional testing would be required to confirm this result with statistical confidence.

Conclusions

Two conventional SCMs, SF and GGBFS, and two comparable particle sizes of waste glass, Glass 1 and Glass 2, were used as cement replacement materials in cements with high and low levels of alkalis in order to compare the performance of glass to traditional SCMs. The effects of the particle size, surface area and alkalinity were observed. Mass loss of $Ca(OH)_2$ was used as a measure of the pozzolanic and ASR reactions taking place, and the presence of ASR was identified using optical and SEM methods. From the results of this testing program, the following conclusions are drawn:

1. When ground to a particle size comparable to SF, waste glass is less reactive and results in less pozzolanic reaction due to the difference in surface areas, where the SF has a surface area nearly ten times greater than that of the glass.
2. When ground to a particle size comparable to GGBFS, waste glass is equivalently reactive based on the consumption of $Ca(OH)_2$ as a measure of pozzolanic reaction since the surface area of the two materials is similar.
3. Use of low alkali cement results in calcium aluminate hydrate phases which are not present in the equivalent high alkali mixtures.
4. A well-distributed glass ranging in particle sizes from 0.3 to 100 μm does not result in ASR gel formation up to 150 days under normal curing conditions.
5. Agglomerations of fine glass particles can initiate localized ASR. The composition of the reaction products can range from a low Ca/Si C–S–H, which does not tend to fluoresce, to a high alkali, low calcium material which demonstrated physical characteristics similar to ASR gel.
6. The composition and characteristics of reacted agglomerates is not strictly dependent on location or proximity to other agglomerates, alkalinity of the cement, or size of the agglomerate.
7. The composition of the reaction rim surrounding an agglomerate demonstrates a unique composition, and can influence the composition of both the reacted agglomerate and the surrounding paste.

Acknowledgements The authors would like to acknowledge the financial support provided through grants by the National Science and Engineering Research Council and the Department of Civil Engineering, McMaster University. The authors would like to acknowledge the training and technical support provided by members of National Research Council Canada Institute for Research in Construction.

References

1. Dubovoy VS, Gebler SH, Klieger P, Whiting DA. Effects of ground granulated blast-furnace slag on some properties of pastes, mortars, and concretes. In: Frohnsdorff G, editor. Blended cements, ASTM STP 897. Philadelphia: American Society for Testing and Materials; 1986. p. 29–47.
2. Hooton RD. Permeability and pore structure of cement pastes containing fly ash, slag, and silica fume. In: Frohnsdorff G, editor. Blended cements, ASTM STP 897. Philadelphia: American Society for Testing and Materials; 1986. p. 128–43.
3. Malhotra VM, Mehta PK. Pozzolanic and cementitious materials. In: Advance in concrete technology, chaps. 1, 4. New York: Gordon and Breach Publishers; 1996. p. 5, 11, 39.
4. Detwiler RJ, Bhatty JI, Bhattacharja S. Supplementary cementing materials for use in blended cements. Skokie: Research and Development Bulletin RD112T Portland Cement Association; 1996.
5. Cook DJ. Natural pozzolans. In: Swamy RN, editor. Cement replacement materials, vol. 3. London: Surrey University Press; 1986. p. 1–39.

6. Rehan R, Nehdi M. Carbon dioxide emissions and climate change: policy implications for the cement industry. Environ Sci Policy. 2005;8:105–14.
7. World Business Council for Sustainable Development. The Cement Sustainability Initiative. In: Cement Sustainability Initiative. World Business Council for Sustainable Development; 2002. http://www.wbcsd.org/DocRoot/1IBetslPgkEie83rTa0J/cement-action-plan.pdf. Accessed 1 Mar 2010.
8. Meyer C, Baxter S, Jin W. Potential of waste glass for concrete masonry blocks. In: Chong KP, editor. Proceedings of the fourth materials engineering conference. Washington: American Society of Civil Engineering; 1996. p. 666–73.
9. Shao Y, Lefort T, Moras S, Rodriguez D. Studies on concrete containing ground waste glass. Cem Concr Res. 2000;30(1):91–100.
10. Shayan A, Xu A. Value-added utilization of waste glass in concrete. Cem Concr Res. 2004;34:81–9.
11. Laldji S, Tagnit-Hamou A. Glass frit for concrete structures: a new, alternative cementitious material. Can J Civ Eng. 2007;34:793–802.
12. Meyer C, Egosi N, Andela C. Concrete with waste glass as aggregate. In: Proceedings of the international symposium concrete technology unit of ASCE and University of Dundee, Dundee; 2001. p. 179–87.
13. Polley C, Cramer SM, de la Cruz RV. Potential for using waste glass in Portland cement concrete. J Mater Civ Eng. 1998;10:210–9.
14. Day RL, Shi C. Influence of the fineness of pozzolan on the strength of lime natural-pozzolan cement pastes. Cem Concr Res. 1994;24:1485–91.
15. Shi C, Day RL. Comparison of different methods for enhancing reactivity of pozzolans. Cem Concr Res. 2001;31:813–8.
16. Shi C, Wu Y, Riefler C, Wang H. Characteristics and pozzolanic reactivity of glass powders. Cem Concr Res. 2005;35:987–93.
17. Schwarz N, Neithalath N. Influence of a fine glass powder on cement hydration: comparison to fly ash and modeling the degree of hydration. Cem Concr Compos. 2008;30:486–96.
18. Dyer TD, Dhir RK. Chemical reactions of glass cullet used as cement component. J Mater Civ Eng. 2001;13:412–7.
19. Diamond S, Thaulow N. A study of expansion due to alkali–silica reaction as conditioned by the grain size of the reactive aggregate. Cem Concr Res. 1974;4:591–607.
20. Jin W, Meyer C, Baxter S. "Glascrete"—concrete with glass aggregate. ACI Mater J. 2000;97:208–13.
21. Pike RG, Hubbard D, Insley H. Mechanisms of alkali-aggregate reaction. ACI J Proc. 1955;52:13–34.
22. Tang M-S, Xu Z-Z, Han S-F. Alkali reactivity of glass aggregate. Durab Build Mater. 1987;4:377–85.
23. Struble LJ, Diamond S. Swelling properties of synthetic alkali silica gels. J Am Ceram Soc. 1981;64(11):652–5.
24. Jin W. Alkali–silica reaction in concrete with glass aggregate—a chemo-physico-mechanical approach. PhD thesis, Columbia University, New York; 1998.
25. Vessalas K, Thomas PS, Ray AS, Guerbois J-P, Joyce P, Haggman J. Pozzolanic reactivity of the supplementary cementitious material pitchstone fines by thermogravimetric analysis. J Therm Anal Calorim. 2009;97:71–6.
26. Kosmatka SH, Kerkhoff B, Panarese WC, MacLeod NF, McGrath RJ. Design and control of concrete mixtures. 7th ed. Ottawa: Cement Association of Ottawa; 2002.
27. Pane I, Hansen W. Investigation of blended cement hydration by isothermal calorimetry and thermal analysis. Cem Concr Res. 2005;35:1155–64.
28. Bhatty JI. A review of the application of thermal analysis to cement-admixture systems. Thermochim Acta. 1991;189:313–50.
29. Ramachandran VS. Thermal analysis. In: Ramachandran VS, Beaudoin JJ, editors. Handbook of analytical techniques in concrete science and technology. Park Ridge: Noyes Publications; 2001. p. 127–73.
30. Wang KS, Lin KL, Lee TY, Tzeng BY. The hydration characteristics when C_2S is present in MSWI fly ash slag. Cem Concr Compos. 2004;26:323–30.
31. Taylor HFW. Cement chemistry. Toronto: Academic Press; 1990.
32. El Elaouni B, Benkaddour M. Hydration of C_3A in the presence of $CaCO_3$. J Therm Anal. 1997;48:893–901.
33. Alarcon-Ruiz L, Platret G, Massieu E, Ehrlacher A. The use of thermal analysis in assessing the effect of temperature on a cement paste. Cem Concr Res. 2005;35:609–13.
34. Marsh BK, Day RL, Bonner DG. Strength gain and calcium hydroxide depletion in hardened cement pastes containing fly ash. Mag Concr Res. 1986;38:23–9.
35. Chaipanich A, Nochaiya T. Thermal analysis and microstructure of Portland cement–fly ash–silica fume pastes. J Therm Anal Calorim. 2010;99:487–93.
36. Ramachandran VS, Paroli RM, Beaudoin JJ, Delgado AH. Handbook of thermal analysis of construction materials. Norwich: William Andrew Publishing/Noyes; 2002.
37. Midgley AJ. The determination of calcium hydroxide in set Portland cements. Cem Concr Res. 1979;9:77–82.
38. Natesaiyer K, Hover KC. Insitu identification of ASR products in concrete. Cem Concr Res. 1988;18:455–63.
39. ASTM International. C856-04: standard practice for petrographic examination of hardened concrete. West Conshohocken: ASTM International; 2004.
40. Suwito A, Jin W, Xi Y, Meyer C. A mathematical model for the pessimum size effect of ASR in concrete. Concr Sci Eng. 2002;4:23–34.
41. Prezzi M, Monteiro PJM, Sposito G. Alkali–silica reaction—part 2: the effect of chemical admixtures. ACI Mater J. 1998;95:3–10.
42. Urhan S. Alkali silica and pozzolanic reactions in concrete. Part 1: interpretation of published results and an hypothesis concerning the mechanism. Cem Concr Res. 1987;17:141–52.
43. Diamond, S. Chemistry and other characteristics of ASR gels. In: Proceedings of the 11th international conference on alkali-aggregate reaction, Quebec; 2000. p. 31–9.
44. Scrivener KL, Monteiro PJM. The alkali–silica reaction in a monolithic opal. J Am Ceram Soc. 1994;77:2849–56.
45. Diamond S, Sahu S, Thaulow N. Reaction products of densified silica fume agglomerates in concrete. Cem Concr Res. 2004;34:1625–32.
46. Dhir RK. Pulverized-fuel ash. In: Swamy RN, editor. Concrete technology and design volume 3, cement replacement material. Glasgow: Surrey University Press; 1986. p. 197–255.
47. Mehta PK. Influence of fly ash characteristics on the strength of Portland–fly ash mixtures. Cem Concr Res. 1985;15:669–74.
48. Pal SC, Mukherjee A, Pathak SR. Investigation of hydraulic activity of ground granulated blast furnace slag in concrete. Cem Concr Res. 2003;33:1481–6.
49. Shi C. Steel slag—its production, processing, characteristics, and cementitious properties. J Mater Civ Eng. 2004;16:230–6.
50. Lawrence P, Cyr M, Ringot E. Mineral admixtures in mortars effect of type, amount, and fineness of fine constituents on compressive strength. Cem Concr Res. 2005;35:1092–105.
51. Diamond S. Alkali silica reactions—some paradoxes. Cem Concr Compos. 1997;19:391–401.
52. Garci Jeunger MC, Jennings HM. Effects of high alkalinity on cement pastes 98-M28. ACI Mater J. 2001;98:251–5.